International Journal of Advanced Trends in Computer Applications
www.ijatca.com

Viscous Flow over an Exponentially Stretching Sheet with Hall, Thermophoresis and Viscous Dissipation Effects

[1]D. Srinivasacharya, [2]P. Jagadeeshwar
[1,2]Department of Mathematics,
National Institute of Technology, Warangal-506004, Telangana, India
[1]*dsrinivasacharya@yahoo.com*, [2]*jagadeeshwar.pashikanti@gmail.com*

Abstract: *The viscous fluid flow past a sheet, stretching exponentially, is investigated under the influence of thermophoresis, Hall currents and viscous dissipation. The coupled nonlinear equations governing the flow are transformed to nonlinear ordinary differential equations. The successive linearization method is implemented to linearize the nonlinear ordinary differential equations. The obtained linearized system is solved using Chebyshev collocation method. The influences of the various flow governing physical parameters on the velocity components, temperature and concentration are presented graphically and analysed. Also, the skin frictions in x- and z-directions are computed and presented in the tabular form.*

Keywords: Hall Current, Thermophoresis and Viscous Dissipation.

I. INTRODUCTION

The study of flow, heat and mass transfer over stretching surface has received considerable attention of the researchers due to its important applications in crystal growth, paper production, food processing, wire drawing, glass fiber, filaments spinning, continuous casting etc. Ever since Sakiadis (1961) initiated the study the flow due to a stretching sheet, several researchers, to mention a few Rohni *et al*. (2013), Bhattacharya and Layek (2014), Lare (2015), Mahanthesh *et al.* ((2017) considered this flow problem for various geometries with different physical conditions.

In recent years, the researchers are attracted to investigate the Hall current effect on MHD flows in view of its spreading applications in electric transformers, power generators, refrigeration coils, power pumps, flight MHD, Hall accelerators, thermal energy storage, electronic system cooling, cool combustors etc. Sahoo and Poncet (2011) presented the effect of magnetic field and partial slip on the flow and heat transfer over a sheet distending exponentially. Nadeema *et al.* (2012) studied the significance of magnetic field on a Casson fluid flow over permeable exponential shrinking sheet. Mukhopadhyay (2013) contemplated the impact of slip boundary condition and magnetic field on the flow and heat transfer phenomena towards a permeable sheet stretching exponentially. Krishnamurthy *et al.* (2015) focused on the flow of a nanofluid over an exponentially stretching surface by considering magnetic and viscous dissipation effects. Hayat *et al.* (2016) studied the 3D MHD flow of viscous fluid saturated porous medium over a surface stretching exponentially. Mabood *et al.* (2017) analyzed the significance of thermal radiation and magnetic field on the flow of a viscous fluid over an exponentially elongating sheet. Recently, Srinivasacharya and Shafeeurrahman (2017) reported the Hall and ion slip effects on the mixed convection flow of a nanofluid between two concentric cylinders.

The mechanism of migrating the small particles in the direction of decreasing thermal gradient is thermophoresis. It is quite significant in radioactive particle deposition in nuclear reactor safety simulations, aerosol particle sampling, deposition of silicon thin films etc. Goldsmith and May (1966) were the first to estimate the thermophoretic velocity in one-dimensional flow. Uddin *et al.* (2012) studied the thermophoresis and magnetic field effect on the flow over a linearly stretching sheet. Shehzad *et al.* (2013) analyzed the effects of magnetic field, radiation, thermoporesis and joule heating effects on the flow of

Jeffrey fluid over a linearly stretched surface. Reddy (2014) investigated the impact of thermophoresis and variable thermal conductivity on MHD viscous fluid flow over an inclined surface. Sandeep and Sulochana (2015) studied the nanofluid flow over an exponentially stretching porous sheet immersed in a porous medium in the presence of thermophoresis, radiation and magnetic field.

The process of transforming the energy taken from the motion of the fluid by the viscosity into internal energy, which is partially irreversible, is referred to as viscous dissipation. Gebhart (1962) considered the significance of viscous dissipation on the natural convection. Wong *et al.* (2012) investigated viscous dissipation effect on the steady viscous fluid flow over a permeable sheet stretching/shrinking exponentially. Das (2014) investigated the effect of viscous dissipation of chemically reacting second grade fluid on MHD flow past a stretching sheet. Megahed (2015) reported the flow of Casson thin film over an unsteady stretching sheet in the presence of viscous dissipation and velocity slip. Adeniyan and Adigun (2016) reported that increasing the values of Eckert number and Magnetic parameter, thermal boundary layer thickness is increasing.

Therefore, motivated by the above investigations, an attempt is made to study the viscous dissipation, thermophoresis, velocity slip at the surface, suction /injection and combined buoyancy effects on the flow over an exponential stretching sheet in the presence of Hall currents.

II. MATHEMATICAL FORMULATION

Consider a steady, laminar, incompressible and electrically conducting viscous fluid flow over a stretching sheet. Let the temperature and concentration of the sheet and ambient medium are $T_w(\tilde{x})$ and $C_w(\tilde{x})$ and C_∞ and T_∞, respectively. The Cartesian coordinate system is considered with the positive $\tilde{x}$-axis is along the sheet and $\tilde{y}$-axis is perpendicular to the sheet. The sheet is stretching with the velocity $U_*(\tilde{x}) = U_0\, e^{\tilde{x}/L}$ where $\tilde{x}$ is the distance from the slit, L is the scaling parameter and U_0 is reference velocity. A magnetic field of strength $B(\tilde{x}) = B_0\, e^{\tilde{x}/2L}$, where B_0 is the constant magnetic field, is applied orthogonal to the sheet without neglecting the influence of Hall current. The assumption of small magnetic Reynolds number allows neglecting the induced magnetic field in contrast to applied magnetic field, due to which the flow becomes three dimensional. The slip velocity and suction/injection velocity at the surface of the sheet are assumed as $N(\tilde{x})=N_0\, e^{-\tilde{x}/2L}$ and $V_*(\tilde{x}) = V_0\, e^{\tilde{x}/2L}$, respectively, where N_0 is the velocity slip factor and V_0 is the strength of suction/injection. Hence, the equations governing the flow are given by

$$\frac{\partial \tilde{u}_x}{\partial \tilde{x}} + \frac{\partial \tilde{u}_y}{\partial \tilde{y}} = 0 \tag{1}$$

$$\tilde{u}_x \frac{\partial \tilde{u}_x}{\partial \tilde{x}} + \tilde{u}_y \frac{\partial \tilde{u}_x}{\partial \tilde{y}} = \nu \frac{\partial^2 \tilde{u}_x}{\partial \tilde{y}^2} + g\, \beta_T (\tilde{T} - T_\infty) + g\, \beta_C (\tilde{C} - C_\infty) - \frac{\sigma B^2}{\rho (1+\beta_h^2)} (\tilde{u}_x + \beta_h \tilde{u}_z) \tag{2}$$

$$\tilde{u}_x \frac{\partial \tilde{u}_z}{\partial \tilde{x}} + \tilde{u}_y \frac{\partial \tilde{u}_z}{\partial \tilde{y}} = \nu \frac{\partial^2 \tilde{u}_z}{\partial \tilde{y}^2} + \frac{\sigma B^2}{\rho (1+\beta_h^2)} (\beta_h \tilde{u}_x - \tilde{u}_z) \tag{3}$$

$$\tilde{u}_x \frac{\partial \tilde{T}}{\partial \tilde{x}} + \tilde{u}_y \frac{\partial \tilde{T}}{\partial \tilde{y}} = \alpha \frac{\partial^2 \tilde{T}}{\partial \tilde{y}^2} + \frac{\mu}{\rho\, c_p} \left[\left(\frac{\partial \tilde{u}_x}{\partial \tilde{y}} \right)^2 + \left(\frac{\partial \tilde{u}_z}{\partial \tilde{y}} \right)^2 \right] \tag{4}$$

$$\tilde{u}_x \frac{\partial \tilde{C}}{\partial \tilde{x}} + \tilde{u}_y \frac{\partial \tilde{C}}{\partial \tilde{y}} = D \frac{\partial^2 \tilde{C}}{\partial \tilde{y}^2} - \frac{\partial}{\partial y} \left[V_{\tilde{T}} (\tilde{C} - C_\infty) \right] \tag{5}$$

where $\tilde{u}_x, \tilde{u}_y, \tilde{u}_z$ are the velocity components, $\tilde{C}$ and $\tilde{T}$ are the concentration and temperature, β_h is Hall parameter, g , and c_p are the acceleration due to gravity, specific heat at the constant pressure, ρ and μ are the density and viscosity of the fluid, D is the mass diffusivity and $V_{\tilde{T}}$ is the thermophoretic velocity, β_T and β_C are the coefficient of thermal and solutal expansions, respectively and σ is electrical conductivity.

The term $V_{\tilde{T}}$ in (5) can be written as (Talbot *et al.* (1980))

$$V_{\tilde{T}} = -\frac{\nu\, k_t}{T_r}\frac{\partial \tilde{T}}{\partial \tilde{y}} \quad (6)$$

where T_r is the reference temperature and k_t is the thermophoretic coefficient.

The conditions on the boundary are

$$\left.\begin{aligned} &\tilde{u}_x = U_0 e^{\frac{\tilde{x}}{L}} + \nu N_0 e^{\frac{\tilde{x}}{2L}}\frac{\partial \tilde{u}_x}{\partial \tilde{y}},\ \tilde{u}_y = -V_0 e^{\frac{\tilde{x}}{2L}}, \tilde{u}_z = 0, T = T_w,\ C = C_w \quad \text{at} \quad \tilde{y} = 0 \\ &(\tilde{u}_x, \tilde{u}_z) \to 0,\ \tilde{T} \to T_\infty,\ \tilde{C} \to C_\infty \quad \text{as} \quad \tilde{y} \to \infty \end{aligned}\right\} \quad (7)$$

Substituting the following similarity transformations

$$\left.\begin{aligned} &\tilde{y} = y\sqrt{\frac{2\nu L}{U_0}} e^{\frac{-\tilde{x}}{2L}},\quad \psi = \sqrt{2\nu L U_0} e^{\frac{\tilde{x}}{2L}} F,\quad \tilde{u}_x = U_0 e^{\frac{\tilde{x}}{L}} F',\quad \tilde{u}_y = -\sqrt{\frac{\nu U_0}{2L}}\, e^{\frac{\tilde{x}}{2L}} (F + yF'), \\ &\tilde{u}_z = U_0 e^{\frac{\tilde{x}}{L}} W,\quad \tilde{T} = T_\infty + T_0\, e^{\frac{2\tilde{x}}{L}} T,\quad \tilde{C} = C_\infty + C_0\, e^{\frac{2\tilde{x}}{L}} C \end{aligned}\right\} \quad (8)$$

into the Eqs. (1) – (5) , we obtain

$$F''' - 2F'^2 + FF'' + 2Ri(T + \mathrm{B}C) - \frac{H_a}{1+\beta_h^2}(F' + \beta_h W) = 0 \quad (9)$$

$$W'' - 2F'W + FW' + \frac{H_a}{1+\beta_h^2}(\beta_h F' - W) = 0 \quad (10)$$

$$T'' + Pr(FT' - 4F'T) + Ec\, Pr\, (W'^2 + F''^2) = 0 \quad (11)$$

$$C'' + Sc(FC' - 4F'C) - Sc\, \tau\left(T'C' + C\, T''\right) = 0 \quad (12)$$

The conditions (7) reduce to

$$\left.\begin{aligned} &F(y) = S,\ F'(y) = 1 + \lambda F''(y),\ W(y) = 0,\ T(y) = 1,\ C(y) = 1 \ \text{at} \quad y = 0 \\ &F'(y) \to 0,\ W(y) \to 0,\ T(y) \to 0,\ C(y) \to 0 \ \text{as} \quad y \to \infty \end{aligned}\right\} \quad (13)$$

where the prime denotes derivative with respect to y, $Pr = \upsilon/\alpha$ and $Sc = \upsilon / D$ are the Prandtl number and the Schmidt number, respectively, $Re = U_0L/\upsilon$, $Gr = g\beta_T T_0 L^3/\upsilon^2$, $Ri = Gr/Re^2$ are the Reynold's, Grashof number and Richardson numbers respectively, $H_a = 2L\sigma B_0^2/\rho U_0$ is the constant magnetic induction, $\lambda = N_0\sqrt{\nu U_0 / 2L}$ is the velocity slip parameter, $S = V_0\sqrt{2L/\nu U_0}$ is the suction/injection parameter ($S > 0$ for suction and $S < 0$ for injection), $Ec = U_0^2/c_pT_0$ is the Eckert number, $\tau = k_t(T_w - T_\infty)$ is the thermophoretic parameter (The surface is cold for $\tau > 0$ and hot for $\tau < 0$ Mills *et al.* (1984); Tsai (1999)) and $\mathrm{B} = \beta_c C_0/\beta_T T_0$ is the buoyancy ratio.

The non-dimensional skin friction in $\tilde{x}$-direction $C_{F\tilde{x}} = 2\tau_{w\tilde{x}}/\rho U_*^2$, skin-friction in $\tilde{z}$ - direction $C_{F\tilde{z}} = 2\tau_{w\tilde{z}}/\rho U_*^2$, the local Nusselt number $Nu_{\tilde{x}} = \tilde{x}\, q_w/\kappa(T_w - T_0)$, and local Sherwood number $Sh_{\tilde{x}} = \tilde{x}\, q_m/\kappa(C_w - C_0)$, are given by

$$\frac{\sqrt{Re_x}}{\sqrt{2x/L}} C_{F\tilde{x}x} = F''(x,0),\ \frac{\sqrt{Re_x}}{\sqrt{2x/L}} C_{F\tilde{z}x} = W'(x,0),$$
$$\frac{Nu_x}{\sqrt{x/2L}\sqrt{Re_x}} = -T'(x,0) \ \text{and} \ \frac{Sh_x}{\sqrt{x/2L}\sqrt{Re_x}} = -C'(x,0) \quad (14)$$

where $Re_x = xU_*(x)/\upsilon$ is the local Reynolds number.

III. NUMERICAL SOLUTION

To linearize the nonlinear system of equations (9) - (12), successive linearization method ((2006), (2011)) is implemented.
For this, it is assumed that

$$F(y) = F_s(y) + \sum_{i=0}^{s-1} F_i(y),\ W(y) = W_s(y) + \sum_{i=0}^{s-1} W_i(y),$$
$$T(y) = T_s(y) + \sum_{i=0}^{s-1} T_i(y),\ C(y) = C_s(Y) + \sum_{i=0}^{s-1} C_i(y) \quad (15)$$

where $F_s(y)$, $W_s(y)$, $T_s(y)$ and $C_s(y)$ $(s = 1,2,3,...)$ are functions to be detrmined and $F_i(y)$, $W_i(y)$, $T_i(y)$ and $C_i(y)$ $(i \geq 1)$ are known from the previous iteration.

Substituting Eq. (15) into Eqs. (9) – (12) , we get the following linearized version of the equations

$$F_r\,'''+\chi_{11,s-1}F_s\,''+\chi_{12,s-1}F_r\,'+\chi_{13,s-1}F_s-\left(\frac{H_a\beta_h}{1+\beta_h^2}\right)W_s+2\;Ri\;(T_s+\mathrm{B}\;\;C_s)=\zeta_{1,s-1} \tag{16}$$

$$\chi_{21,s-1}F_s\,'+\chi_{22,s-1}F_s+W_s\,''+\chi_{23,s-1}W_s\,'+\chi_{24,s-1}W_s=\zeta_{2,s-1} \tag{17}$$

$$\chi_{31,s-1}F_s\,''+\chi_{32,s-1}F_s\,'+\chi_{33,s-1}F_s+\chi_{34,s-1}W_s\,'+T''+\chi_{35,s-1}T'+\chi_{36,s-1}T=\zeta_{3,s-1} \tag{18}$$

$$\chi_{41,r-1}F_r\,'+\chi_{42,s-1}F_s+\chi_{43,s-1}T_s\,''+\chi_{44,s-1}T_s\,'+C_s\,''+\chi_{45,s-1}C_s\,'+\chi_{46,s-1}C_s=\zeta_{4,s-1} \tag{19}$$

where $\chi_{lk,s-1}$ and $\zeta_{l,i-1}$, (*l = 1, 2, 3, 4, k = 1, 2, 3, 4, 5, 6*) are in terms F_i, W_i, T_i and C_i, (*i = 1,2,..., s-1*) and their derivatives.

The corresponding conditions on the sheet are

$$F_s(0)=0,\;\lambda F_s\,''(0)-F_s\,'(0)=0,F_s\,'(\infty)=0,W_s(0)=0,$$
$$W_s(\infty)=0,T_s(0)=0,T_s(\infty)=0,C_s(0)=0,C_s(\infty)=0 \tag{20}$$

The linearized equations (16) to (19) along with the boundary conditions (20), are solved using Chebyshev collocation method (2007). In this method, the functions $F_r(y)$, $W_r(y)$, $T_r(y)$ and $C_r(y)$ and their derivative approximated by the Chebyshev polynomials and these polynomials are collocated at $J+1$ Gauss-Lobatto points in the interval $[-1,1]$ and then ubstituting them into the equations (17)-(22) leads to a system of algebraic equations. Writing the boundary conditions in terms of Chebyshev polynomials at the collocation points, incorporating them in the system and then solving the resultant matrix system, we obtain the solution.

Choosing the initial approximation $F_0(y)$, $W_0(y)$, $T_0(y)$, and $C_0(y)$ satisfy the conditions (13) and solving Eqs. (16) to (19) recursively, we get $F_r(y)$, $W_r(y)$, $T_r(y)$ and $C_r(y)$ ($r \geq 1$) and hence, *F(y), W(y), T(y)* and *C(y)*.

IV. RESULTS AND DISCUSSION

To explain the significant effect of Magnetic parameter, Hall parameters, thermophoresis parameter, Richardson number and Eckert number on the physical quantities of interest, the numerical computations are carried out by assigning B = 0.5, *Pr* = 1.0, β_h = 1.0, τ = 0.3, *Sc* = 0.22, *Ec* = 0.5, *Ri* = 1.0, λ = 1.0, *S* = 0.5, H_a = 2.0, *N* = 100 and *L* = 20 unless otherwise mentioned.

The variations of *F'(y), W(y), T(y)* and *C(y)* for diverse values of magnetic parameter H_a are presented in the Figs. 1(a) – 1(d). It is apparent from the Fig. 1(a), that the tangential velocity *F'(y)* is reducing with an enhancement in H_a. The application of uniform magnetic field orthogonal to flow direction contributes Lorentz force which has the propensity to decelerate the velocity. From Fig. 1(b), it is noticed that the cross-flow velocity vanishes for small values of H_a (i.e. $H_a \to 0$). Higher values of H_a (i. e. $H_a > 0$) produces a Hall current in the flow and subsequently cross flow velocity is created. Further, it is noticed that the enhancement in H_a results in gradual enhancement in the cross flow velocity. An escalation in the value of H_a escalate the temperature and concentration as depicted in the Figs. 1(c) - 1(d)

The influence of Hall parameter β_h on *F'(y), W(y), T(y)* and *C(y)* is shown in Figs 2(a) – 2(d). From Fig. 2(a), it is perceived that the velocity *F'(y)* rises with a raise in β_h. Figure 2(b) indicates that *W(y)* enhances with an enhancement in β_h. This is in tune with the fact that the Hall currents produce cross flow velocity. The *T(y)* and *C(y)* are reducing with an enhancement in β_h as presented in Figs 2(c) and 2(d).

The impact of τ on the tangential velocity *F'(y)*, transverse velocity *W(y)*, temperature *T(y)* and concentration *C(y)* is depicted in the Figs. 3(a) – 3(d). These figures reveal that *F'(y)* is diminishing with increment in the values τ. The same trend is seen for the *W(y)* as shown in the Fig. 3(b). From the Fig. 3(c), it is witnessed that *T(y)* is enhancing with enhancement in *τ*. Further, *C(y)* is lessened with escalating values of *τ*.

The behavior of *F'(y), W(y), T(y)* and *C(y)* with the Eckert number *Ec* is demonstrated in the Figs. 4(a) – 4(d). From Figs. 4(a) and 4(b), it is perceived that both the velocities are rising with an escalation in the value of *Ec*. It is apparent from the Fig. 4(c) that the temperature rises with increasing value *Ec*, . Figure 4(d) shows that concentration is reducing with increase in the value of *Ec*. It is obvious from the figures that the impact of *Ec* on the profiles is very less.

The influence of Richardson number *Ri*, Hall parameter β_h, magnetic parameter H_a, , thermophoretic parameter *τ*, Eckert number *Ec* and slip parameter λ on the heat transfer (*-T'(0)*) and mass transfer (*-C'(0)*) coefficients against *S* are depicted in the Figs. (5) to (10). It is understood from the figures 5(a) and 5(b) that *-T'(0)* and *-C'(0)* are improving with the improvement in *Ri* and *S*. It is evident from Fig. 6(a) and Fig. 6(b) that, the heat transfer and mass transfer phenomena are increasing with a rise in the value of Hall parameter β_h. It is identified from Figs. 7(a) and Fig. 7(b) that, heat transfer and mass transfers coefficients are diminishing with enhancement in the value of the H_a. Further, it is clear from the figures that the variation in the mass transfer is more to that of heat transfer. -*T'(0)* is decreasing with the increasing value of τ as presented in the Fig. 8(a). -*C'(0)* is increasing when the value of τ is raised as shown in the Fig. 8(b). But, the amount of mass transfer from the sheet to the fluid is very high when compared that decrease in heat transfer from the sheet to fluid. It is depicted from Fig. 9(a) that heat transfer coefficient is decreasing with increase in the values of *Ec*. But, an opposite trend is observed for mass transfer rate as shown in 9(b). Further, it is identified that mass transfer rate is decreasing with increasing values of *Ec* after S = 1.4. It is seen from the Fig. 10(a) that the heat transfer rate is decreasing with increase in λ. Further, mass transfer rate is decreasing with increase in the value of λ as presented in Fig. 10(b).

The behavior of skin friction in x- and z- directions (i.e. *F''(0)* and *W'(0))* for diverse values of slip parameter λ, Hall parameter β_h, magnetic parameter H_a, Richardson number *Ri*, Eckert number *Ec* and thermophoretic parameter τ are presented in Table (1). It is apparent from the table that the *F''(0)* is increasing and *W'(0)* reducing with λ. The skin-frictions in x- and z-directions are increasing in the presence of β_h,. Since the transverse velocity vanishes when β_h = 0, there is no skin-friction in $\tilde{z}-$direction. As the magnetic parameter enhances, *F''(0)* is decreasing and *W'(0)* is increasing, F''(0) and *W'(0)* are increasing with increase in *Ri*. On other hand, Eckert number *Ec* increases both the skin-frictions. It is noticed that, both *F''(0)* and *W'(0)* are decreasing with increasing value of τ.

Table 1: Effect of λ, β_h, H_a, *Ri*, *Ec* and τ on *F''(0)* and *W'(0)*

λ	β_h	H_a	*Ri*	*Ec*	τ	*F''(0)*	*W'(0)*
0.0	1.0	2.0	1.0	0.5	0.3	-0.91411137	0.47617496
0.5	1.0	2.0	1.0	0.5	0.3	-0.40508974	0.43196532
1.0	1.0	2.0	1.0	0.5	0.3	-0.26159285	0.41872230
2.0	1.0	2.0	1.0	0.5	0.3	-0.15337319	0.40848340
1.0	0.0	2.0	1.0	0.5	0.3	-0.32860030	0.00000000
1.0	0.1	2.0	1.0	0.5	0.3	-0.32751833	0.06334880
1.0	0.5	2.0	1.0	0.5	0.3	-0.30513773	0.28064884
1.0	2.0	2.0	1.0	0.5	0.3	-0.20049245	0.42829099
1.0	1.0	0.0	1.0	0.5	0.3	-0.13763450	0.00000001
1.0	1.0	0.1	1.0	0.5	0.3	-0.14406720	0.03334707
1.0	1.0	1.0	1.0	0.5	0.3	-0.20217920	0.26244830
1.0	1.0	3.0	1.0	0.5	0.3	-0.31336413	0.51755964
1.0	1.0	2.0	0.0	0.5	0.3	-0.61660061	0.15023781
1.0	1.0	2.0	0.5	0.5	0.3	-0.41196661	0.32493986
1.0	1.0	2.0	1.5	0.5	0.3	-0.13354694	0.48753998
1.0	1.0	2.0	3.0	0.5	0.3	0.18359188	0.63163669
1.0	1.0	2.0	1.0	0.0	0.3	-0.26528503	0.41540314
1.0	1.0	2.0	1.0	0.1	0.3	-0.26454405	0.41606772
1.0	1.0	2.0	1.0	0.6	0.3	-0.26085833	0.41938493
1.0	1.0	2.0	1.0	1.0	0.3	-0.25793402	0.42203084
1.0	1.0	2.0	1.0	0.5	0.0	-0.25881448	0.42180522
1.0	1.0	2.0	1.0	0.5	0.1	-0.25974839	0.42077008
1.0	1.0	2.0	1.0	0.5	0.5	-0.26340638	0.41670467
1.0	1.0	2.0	1.0	0.5	1.0	-0.26780688	0.41179353

V. CONCLUSION

The Hall effect on the flow of viscous fluid over sheet elongating exponentially is studied by taking Thermophoresis and viscous dissipation effects into account. The governing equations are solved using the successive linearization method along with the Chebyshev spectral collocation method.

- An increase in the values of Hall parameter and Eckert number, the tangential velocity is increasing. It is decreasing with the rise in magnetic and thermophoresis parameters. Transverse velocity is increasing with increase in magnetic, Hall parameters and Eckert number and reverse trend for thermophoresis parameter.
- In the presence of magnetic, thermophoresis parameters and Eckert number, temperature is

increasing. The temperature is diminishing with an increment in the value of Hall parameter. The same tendency is observed in the concentration, except for the thermophoresis parameter and Eckert number.

F''(0) decreases with an increase in the value of magnetic and thermophoresis parameters and increasing in all other cases. *W'(0)* is decreasing with increasing value of slip and thermophoresis parameters and increasing in all other cases.

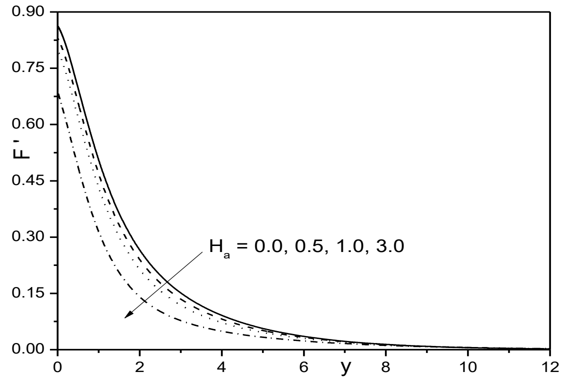

1(a)

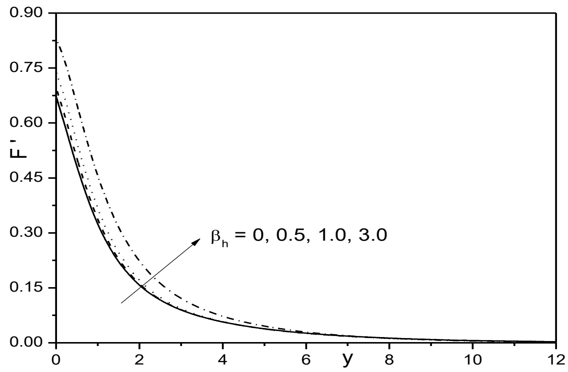

2(a)

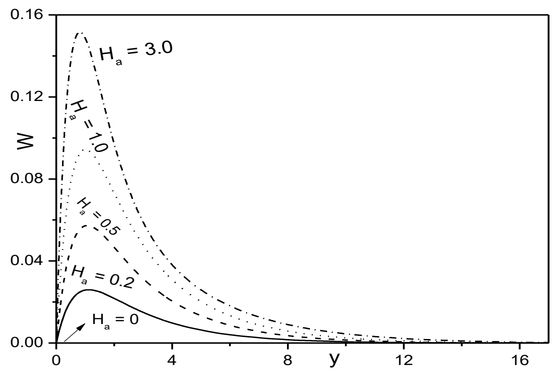

1(b)

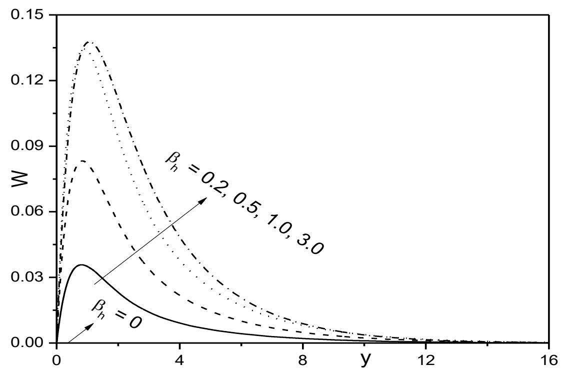

2(b)

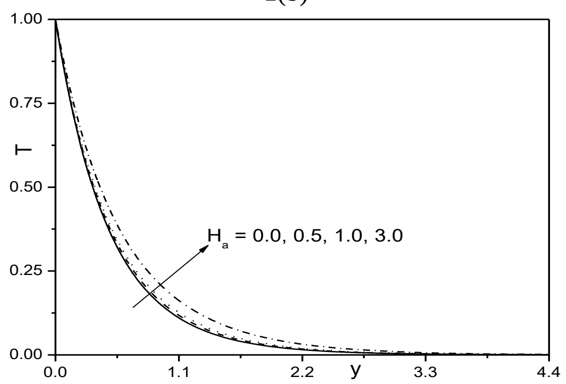

1(c)

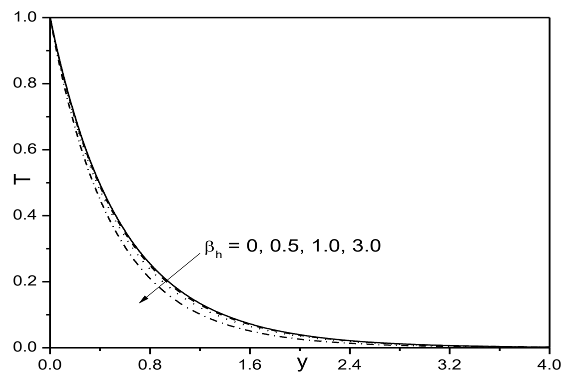

2(c)

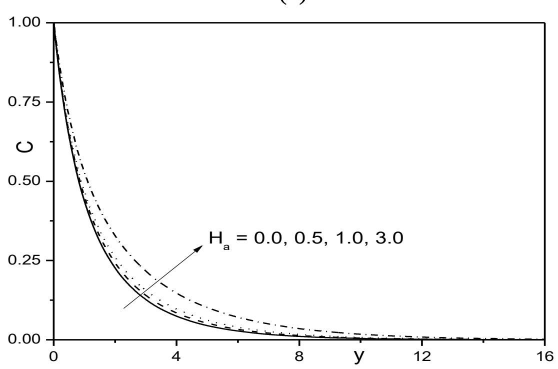

1(d)

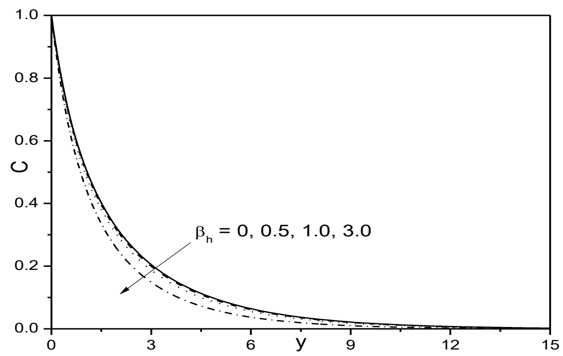

2(d)

Figure 1: Variation of (a) F' (b) W (c) T and (d) C with H_a

Figure 2: Variation of (a) F' (b) W (c) T and (d) C with β_h

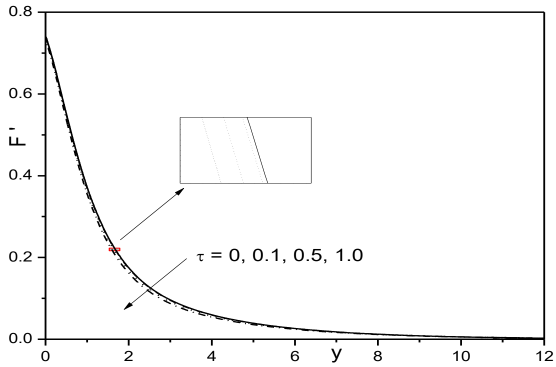

3(a)

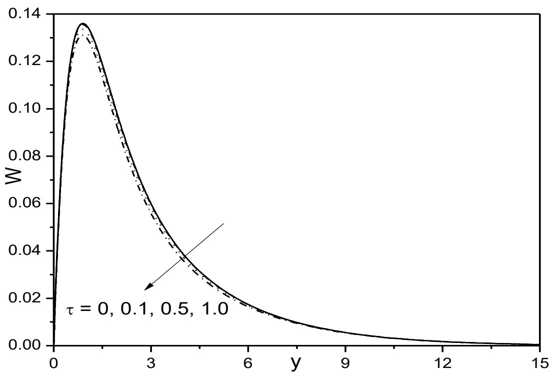

3(b)

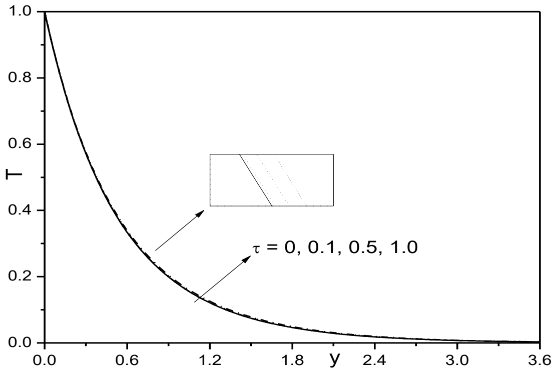

3(c)

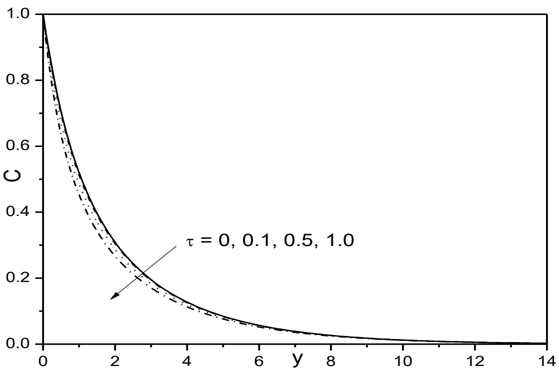

3(d)

Figure 3: Variation of (a) F' (b) W (c) T and (d) C with τ

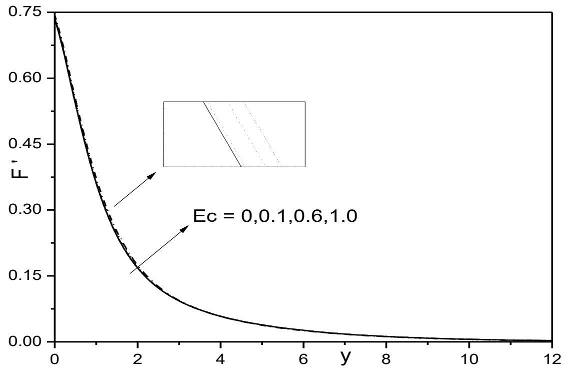

4(a)

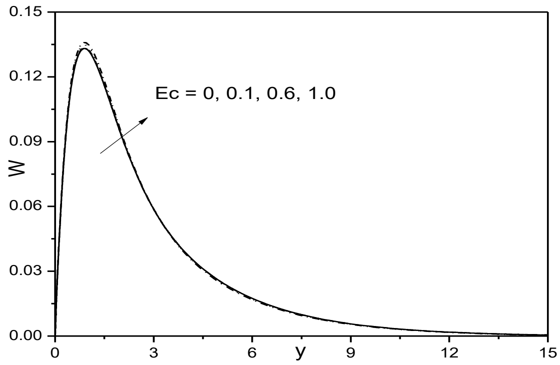

4(b)

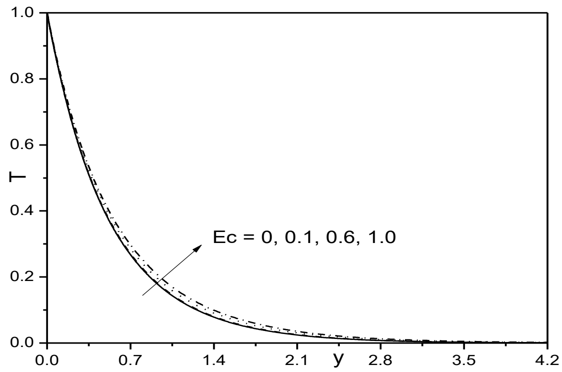

4(c)

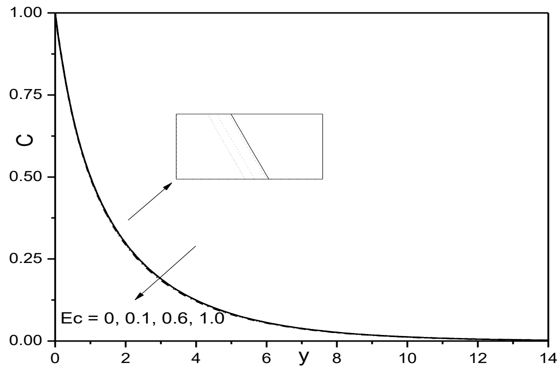

4(d)

Figure 4: Variation of (a) F' (b) W (c) Tand (d) C with Ec

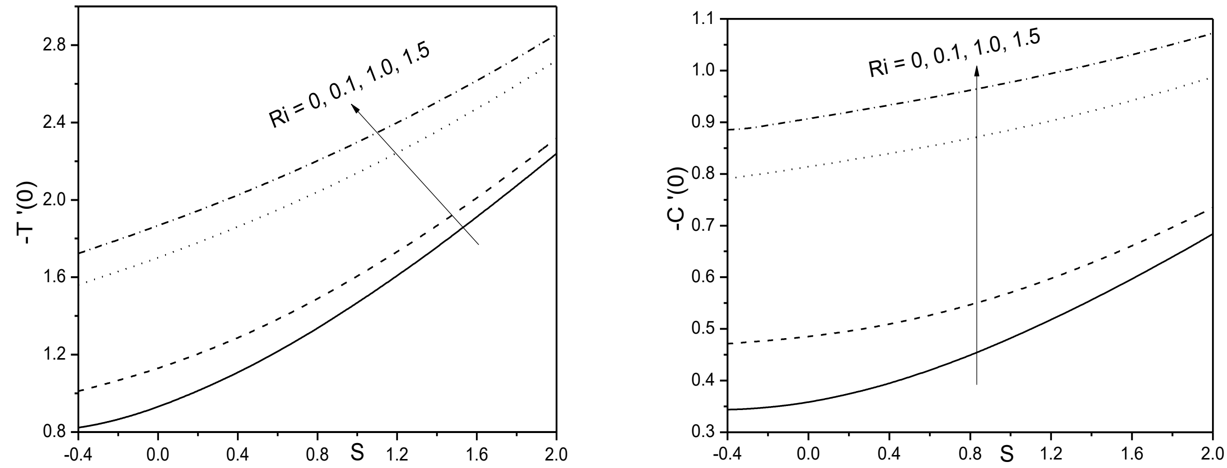

5(a) 5(b)

Figure 5: Variation of (a) –T '(0) and (b) –C '(0) with Ri

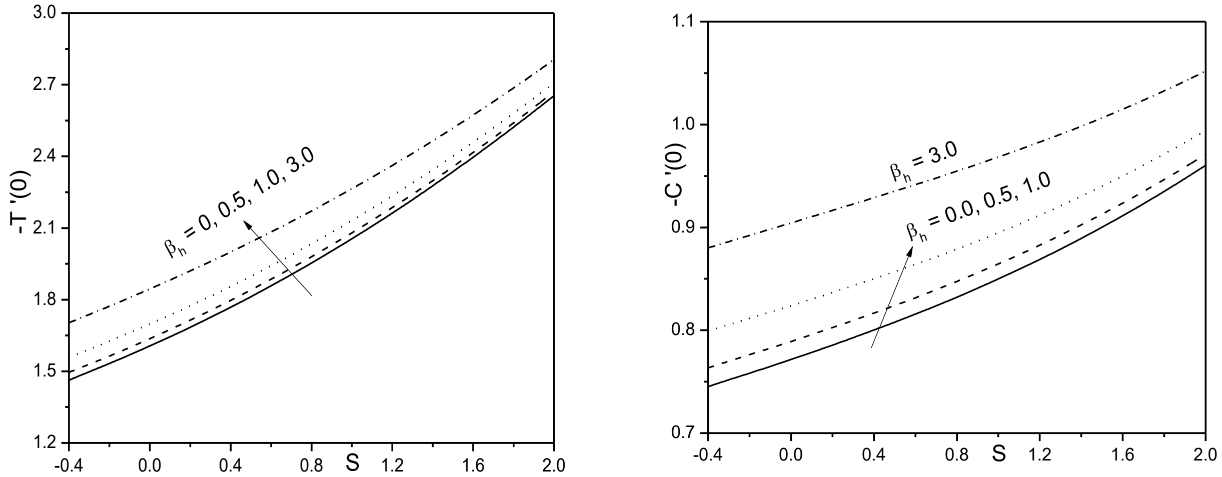

6(a) 6(b)

Figure 6: Variation of (a) –T '(0) and (b) –C '(0) with β_h

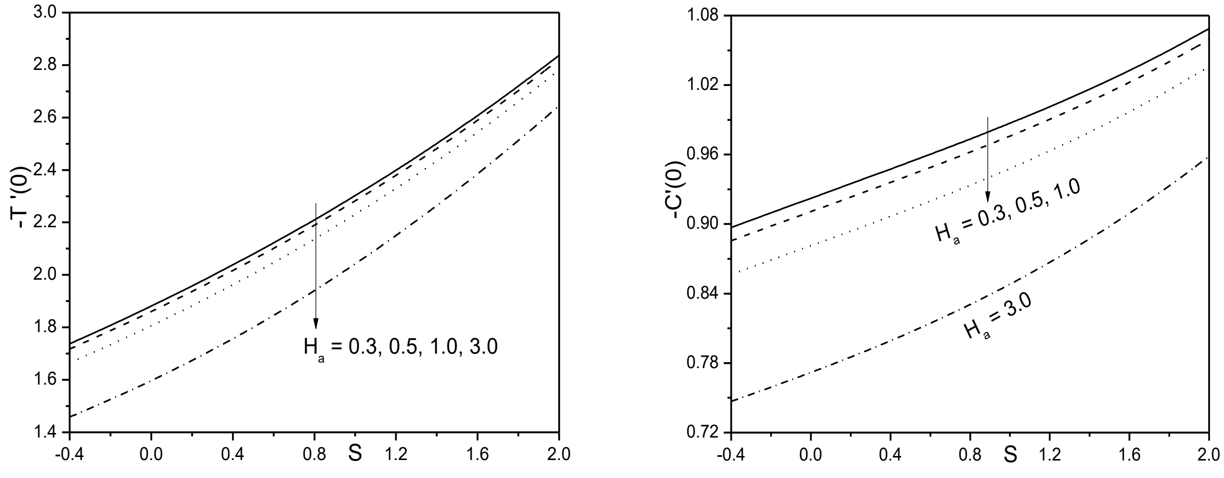

7(a) 7(b)

Figure 7: Variation of (a) –T '(0) and (b) –C '(0) with H_a

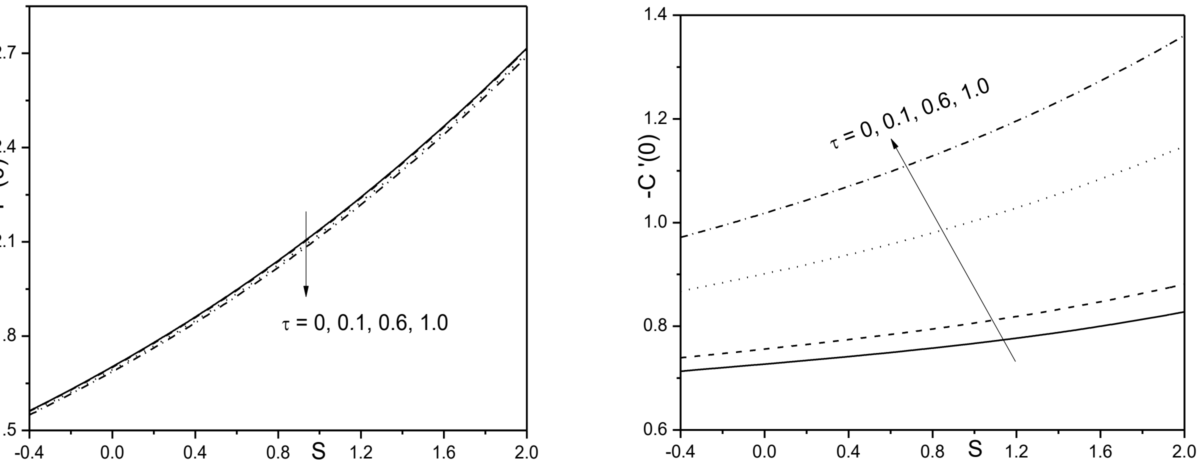

8(a) 8(b)

Figure 8: Variation of (a) –T '(0) and (b) –C '(0) with τ

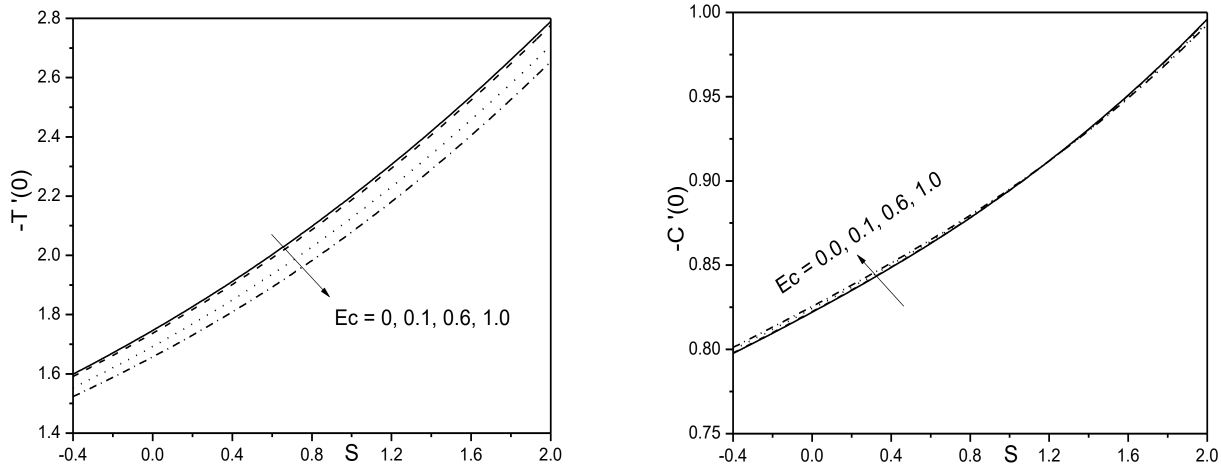

9(a) 9(b)

Figure 9: Variation of (a) –T '(0) and (b) –C '(0) with Ec

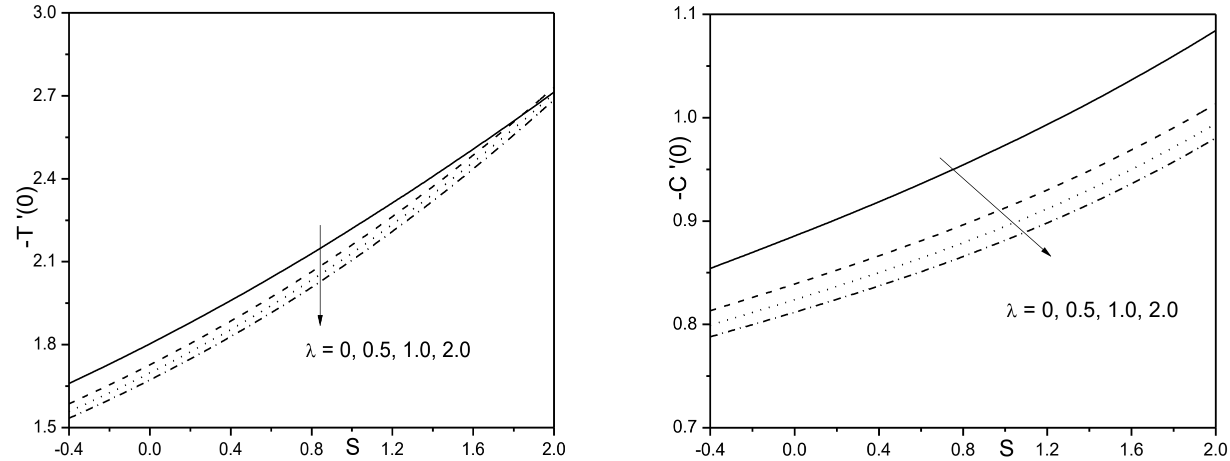

10(a) 10(b)

Figure 10: Variation of (a) –T '(0) and (b) –C '(0) with λ

Conflict of Interest

All authors have equal contribution in this work and declare that there is no conflict of interest for this publication.

References

[1]. Adeniyan, A., & Adigun, J.A. (2016). Similarity Solution of hydromagnetic flow and heat transfer past an exponentially stretching permeable vertical sheet with viscous dissipation, Joulean and viscous heating effects,

Annals of the Faculty of Engineering Hunedoara-International Journal of Engineering. 14(2), 113-120.

[2]. Awad, F.G., Sibanda, P.,. Motsa, S. S., & Makinde, O.D. (2011). Convection from an inverted cone in a porous medium with cross-diffusion effects, Computers and Mathematics with Applications. 61(5), 1431-1441.

[3]. Bhattacharya, K., & Layek, G.C. (2014). Thermal Boundary Layer in Flow due to an Exponentially Stretching Surface with an Exponentially Moving Free Stream, Modelling and Simulation in Engineering. 2014(36).

[4]. Canuto, C., Hussaini, M.Y., Quarteroni, A., & Zang, T. A. (2007). Spectral Methods- Fundamentals in Single Domains, Journal of Applied Mathematics and Mechanics. 87(1).

[5]. Das, K. (2014). Influence of chemical reaction and viscous dissipation on MHD mixed convection flow, Journal of Mechanical Science and Technology. 28(5),1881-1885.

[6]. Gebhart, B. (1962). Effects of viscous dissipation in natural convection, Journal of Fluid Mechanics. 14(2), 225-232.

[7]. Goldsmith, P., & May, F. G. (1966). Diffusiophoresis and thermophoresis in water vapour systems, Aerosol science. 163-194.

[8]. Hayat, T., Shafiq, A., Alsaedi, A., & Shahzad, S. A. (2016). Unsteady MHD flow over exponentially stretching sheet with slip conditions, Applied Mathematics and Mechanics. 37(2), 193-208.

[9]. Krishnamurthy, M.R., Prasannakumara, B. C., Gireesha, B. J. & Gorla, R. S. R. (2015). Effect of viscous dissipation on hydromagnetic fluid flow and heat transfer of nanofluid over an exponentially stretching sheet with fluid-particle suspension, Cogent Mathematics. 2(1).

[10]. Lare, A.I. (2015). Casson fluid flow of variable viscosity and thermal conductivity along exponentially stretching sheet embedded in a thermally stratified medium with exponentially heat generation, Journal of Heat and Mass Transfer Research. 2(2), 63-78.

[11]. Mabood, F., Khan, W.A., & Ismail, A.I.Md. (2017). MHD flow over exponential radiating stretching sheet using Homotopy analysis method, Journal of King Saud University - Engineering Sciences. 29(1), 68-74.

[12]. Mahanthesh, B., Gireesha, B.J., & Gorla, R. S. R. (2017). Unsteady three-dimensional MHD flow of a nano Eyring-Powell fluid past a convectively heated stretching sheet in the presence of thermal radiation, viscous dissipation and Joule heating, Journal of the Association of Arab Universities for Basic and Applied Sciences. 23, 75-84.

[13]. Megahed, A.M. (2015). Effect of slip velocity on Casson thin film flow and heat transfer due to unsteady stretching sheet in presence of variable heat flux and viscous dissipation, Applied Mathematics and Mechanics. 36(10), 1273-1284.

[14]. Mills, A.F., Xu, H., & Ayazi, F. (1984). The effect of wall suction and thermophoresis on aerosol-particle deposition from a laminar boundary layer on a flat plate, International Journal of Heat and Mass Transfer. 27(7), 1110-1113.

[15]. Motsa, S. S., & Shateyi, S. (2011). Successive linearisation solution of free convection non-Darcy flow with heat and mass transfer, Advanced Topics in Mass Transfer. 19, 425-438.

[16]. Mukhopadhyay, S. (2013). Slip effects on MHD boundary layer flow over an exponentially stretching sheet with suction/blowing and thermal radiation, Ain Shams Engineering Journal. 4(3), 485-491.

[17]. Nadeem, S., Ul Haq, R., & Lee, C. (2012). MHD flow of a Casson fluid over an exponentially shrinking sheet, Scientia Iranica. 19(6), 1550-1553.

[18]. Reddy, M.G. (2014). Effects of thermophoresis, viscous Dissipation and Joule heating on steady MHD flow over an inclined radiative isothermal permeable surface with variable thermal conductivity, Journal of Applied Fluid Mechanics. 7(1), 51-61.

[19]. Rohni, A.Md., Ahmad, S., Ismail, A.I.Md., & Pop, I. (2013). Boundary layer flow and heat transfer over an exponentially shrinking vertical sheet with suction, International Journal of Thermal Sciences. 64, 264-272.

[20]. Sahoo, B., & Poncet, S. (2011). Flow and heat transfer of a third grade fluid past an exponentially stretching sheet with partial slip boundary condition, International Journal of Heat and Mass Transfer. 54(23), 5010-5019.

[21]. Sakiadis, B.C. (1961). The Boundary Layer on a Continuous Flat Surface, A.I.Ch.E. Journal. 7(2), 221-225.

[22]. Sandeep, S., & Sulochana, C. (2016). Dual solutions of radiative MHD nanofluid flow over an exponentially stretching sheet with heat generation/absorption, Applied Nanoscience. 6(1), 131-139.

[23]. Shehzad, S.A., Alsaedi, A., & Hayat, T. (2013). Influence of thermophoresis and Joule heaating on the radiative flow of Jeffrey fluid with mixed convection, Brazilian Journal of Chemical Engineering. 30(4), 897-908.

[24]. Srinivasacharya, D., & Shafeeurrahman, Md. (2017). Hall and ion slip effects on mixed convection flow of nanofluid between two concentric cylinders, Journal of the Association of Arab Universities for Basic and Applied Sciences.

[25]. Talbot, L., Cheng, R.K., Schefer, R.W., & Willis, D.R., Thermophoresis of particles in a heated boundary layer, Journal of Fluid Mechanics. 101(4), 737-758.

[26]. Tsai, R. (1999). A simple approach for evaluating the effect of wall suction and thermophoresis on aerosol particle deposition from a laminar flow over a flat plate, International Communications in Heat and Mass Transfer. 26(2), 249-257.

[27]. Uddin, Md.J., Khan, W.A., & Ismail, A.I.Md. (2012). Scaling group transformation for MHD boundary layer slip flow of a nanofluid over a convectively heated stretching sheet with heat generation, Mathematical Problems in Engineering. 2012.

[28]. Wong, S. W., Awang, M.A.O., Ishak, A., & Pop, I. (2012). Boundary layer flow and heat transfer over an exponentially stretching/shrinking permeable sheet with viscous dissipation, Journal of Aerospace Engineering. 27(1), 26-32.